Significant Conformational Changes Associated with Molecular Transport in a Crystalline Solid

Javier Martí-Rujas and Kenneth D. M. Harris*

School of Chemistry, Cardiff University, Park Place, Cardiff CF10 3AT, Wales

Arnaud Desmedt and François Guillaume*

Laboratoire de Physico Chimie Moléculaire, UMR CNRS 5803, Université de Bordeaux 1, 351 cours de la Libération, 33405 Talence Cedex, France

Received: February 3, 2006; In Final Form: April 4, 2006

Confocal Raman microspectrometry has been applied as an in situ probe of the transport of guest molecules along the one-dimensional tunnels in a crystalline urea inclusion compound, under conditions of guest exchange in which "new" guest molecules (pentadecane) are introduced at one end of the tunnel and displace the "original" guest molecules (1,8-dibromooctane). The Raman spectra, recorded as a function of position along the tunnel direction and as a function of time, demonstrate that the transport process is associated with a significant change in the conformational properties of the original (1,8-dibromooctane) guest molecules. In particular, in the boundary region between the original and new guest molecules, there is a substantial increase in the proportion of 1,8-dibromooctane guest molecules that have the gauche end-group conformation. The wider implications of this observation are discussed in relation to fundamental aspects of the molecular transport process in this material.

1. Introduction

There is currently considerable interest in processes that involve transport of molecules or ions through channel or tunnel systems, including those of biological[1−6] and industrial[7,8] importance, and the transport of molecules within nanotubes and nanoporous materials and membranes.[9−14] Studies of appropriate model systems, represented for example by crystalline tunnel systems of well-defined and regular structure, can play an important role in developing an understanding of fundamental aspects of such processes. One such model system is based on conventional urea inclusion compounds,[15−19] in which guest molecules are contained within one-dimensional tunnels with a diameter of ca. 5.5 Å in a crystalline urea host structure[20,21] (Figure 1).

An important feature of urea inclusion compounds is that the urea tunnel structure is stable only when the tunnels are filled with a dense packing of guest molecules. Thus, removal of the guest molecules leads to instantaneous collapse of the "empty" urea tunnel structure, and formation of the pure crystalline phase of urea. Guest exchange therefore cannot be carried out via the empty host tunnel structure (unlike the situation for other host structures, such as zeolites, that are generally stable in the empty form[7,8]). However, as demonstrated previously,[22] provided that the tunnels in the urea host structure remain filled throughout the guest exchange process, the identity of the guest molecules can be changed as a function of time while still maintaining the integrity of the host structure. Such guest exchange can be carried out by inserting new guest molecules at one end of the crystal (by putting it in contact with the liquid of another potential guest), with the original guest molecules expelled from the other end of the crystal, and a net transport of guest molecules occurs in one direction along the host tunnels. To understand details of such guest exchange processes, it is essential to understand the spatial distribution of the two types of guest molecule within the crystal and the variation of the

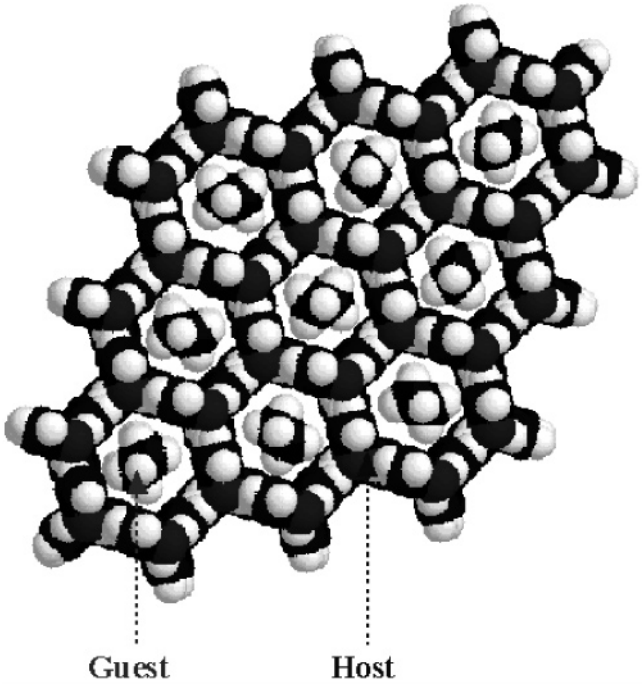

Figure 1. Structure of an alkane/urea inclusion compound showing nine complete tunnels filled with alkane guest molecules (the guest molecules are not actually located from X-ray diffraction data at ambient temperature but have been inserted into the tunnels in the plot in a manner that illustrates orientational disorder).

* Authors for correspondence. E-mail: HarrisKDM@cardiff.ac.uk (K.D.M.H.); f.guillaume@lpcm.u-bordeaux1.fr (F.G.).

10.1021/jp060738o CCC: $33.50
Published on Web 05/13/2006

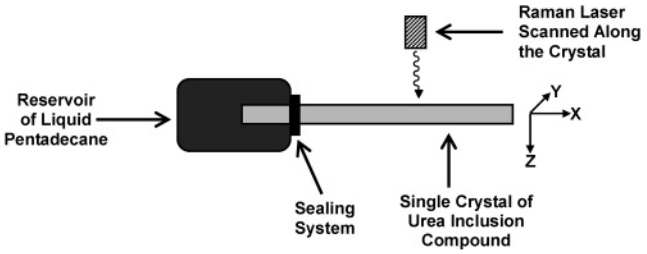

Figure 2. Schematic representation of the experimental assembly for in situ Raman microspectrometry of guest exchange in a urea inclusion compound, comprising the single crystal of the urea inclusion compound (light gray), initially containing 1,8-dibromooctane guest molecules, attached to a reservoir containing liquid pentadecane (dark gray). The laboratory reference frame (*X*, *Y*, *Z*) is also defined.

spatial distribution as a function of time during the process. Recently, it was demonstrated[23] that confocal Raman microspectrometry can be used as an in situ probe of such guest exchange processes (Figure 2), yielding the required information on the spatial distribution of the "original" and "new" guest molecules within the crystal and the time dependence of the spatial distribution.

Our previous studies of guest exchange in urea inclusion compounds[22,23] were focused on the system with 1,8-dibromooctane as the original type of guest molecule and pentadecane as the new type of guest molecule, and focused in particular on the variation in the intensity (in the Raman spectrum) of the C−Br stretching band for the trans end-group conformation [here denoted $\nu(CBr_T)$] of the 1,8-dibromooctane guest molecules as a function of position in the crystal and as a function of time. In independent studies[24] of urea inclusion compounds containing α,ω-dibromoalkane guest molecules [$Br(CH_2)_nBr$; $n = 7-11$], it has been shown by Raman spectroscopy that, under ambient conditions, the trans end-group conformation is predominant, with the percentage of gauche end-groups reported to be ca. 7−13%.

In our previous in situ studies[23] using confocal Raman microspectrometry, we showed that progress of the guest exchange process could be monitored by studying the variation in the intensity of the $\nu(CBr_T)$ band, which decreases in a well-defined manner as the original 1,8-dibromooctane guest molecules are replaced by the new pentadecane guest molecules. We have now extended these previous studies by focusing also on the C−Br stretching band for the gauche end-group conformation [here denoted $\nu(CBr_G)$] of the 1,8-dibromooctane guest molecules, allowing an assessment of possible changes in the conformational properties of the guest molecules as a consequence of the exchange process.

2. Strategy

Previous Raman studies[24] of the 1,8-dibromooctane/urea inclusion compound have shown that the $\nu(CBr_T)$ band is at ca. 660 cm^{-1} and the $\nu(CBr_G)$ band is at ca. 570 cm^{-1}. For pentadecane guest molecules (in the *all*-trans conformation) in the pentadecane/urea inclusion compound, the methyl-rocking vibration $r(CH_3)$ gives a peak at ca. 900 cm^{-1} in the Raman spectrum.[25] The Raman bands due to the urea host structure are identical for both the 1,8-dibromooctane/urea and pentadecane/urea inclusion compounds, and the symmetric C−N stretching vibration $\nu_s(CN)$ of urea gives a very intense band at ca. 1024 cm^{-1}.[24,25] These features in the Raman spectra of urea inclusion compounds are highlighted in Figure 3.

In our previous in situ studies[23] of guest exchange in urea inclusion compounds using confocal Raman microspectrometry,

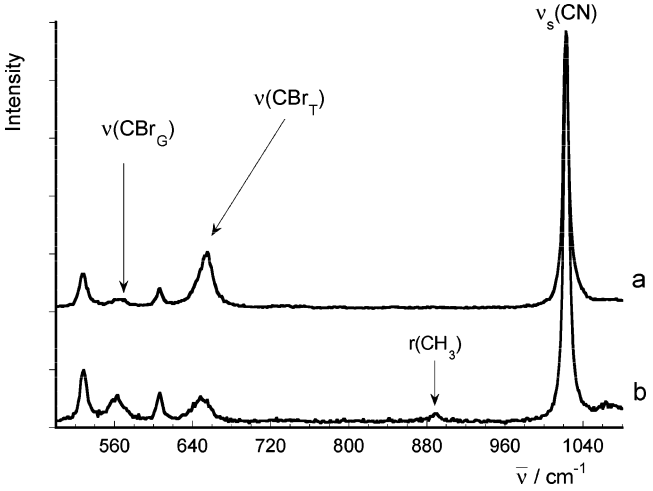

Figure 3. Raman spectra of (a) a crystal of the 1,8-dibromooctane/urea inclusion compound (before guest exchange) and (b) the urea inclusion compound after partial exchange of the 1,8-dibromooctane guest molecules by pentadecane.

the relative amounts of 1,8-dibromooctane and pentadecane guest molecules in different regions of the crystal were assessed by considering the ratio $R = I(CBr_T)/I(CN)$ of the integrated intensities [denoted $I(CBr_T)$ and $I(CN)$, respectively] of the $\nu(CBr_T)$ and $\nu_s(CN)$ bands in the Raman spectrum. Thus, the advancement of the new pentadecane guest molecules through the crystal (and the corresponding loss of the original 1,8-dibromooctane guest molecules) was monitored by considering the variation of R as a function of position in the crystal and as a function of time. In practice, the normalized ratio $R_N = R/R_0$ was used, where R_0 denotes the value of R (averaged over the probed area) for the original crystal of the 1,8-dibromooctane/urea inclusion compound before the start of the guest exchange process (by definition, $R_N = 1$ for the original 1,8-dibromooctane/urea inclusion compound, and $R_N = 0$ would correspond to an inclusion compound containing only pentadecane guest molecules). In the present work, the above ratio R_N is denoted $R_{N,T}$ (to specify that it refers to the relative intensity of the $\nu(CBr_T)$ band).

Our previous studies[23] of $R_{N,T}$ as a function of position (X) along the tunnel direction and as a function of time (t) showed that, at a given value of time, there is an approximately sigmoidal distribution of the original and new guest molecules within the crystal. A typical graph (taken from our current work) of $R_{N,T}$ versus position X at a fixed value of time is shown in Figure 4. The "limiting regions" of the sigmoidal distribution are the 1,8-dibromooctane-rich (high X values; $R_{N,T} \approx 1$) and pentadecane-rich (low X values; $R_{N,T} \approx 0.2$) regions of the crystal. As noted previously[23] and discussed further in section 5, complete guest exchange is not actually observed and the final value of $R_{N,T}$ in the pentadecane-rich regions does not fall to zero. Between these limiting regions, there is a "boundary region" in which the value of $R_{N,T}$ varies significantly with position X along the tunnel (a more detailed discussion of the physical interpretation of the boundary region is given in section 5). Such plots, studied as a function of time, demonstrate that the centroid of the sigmoidal distribution (which clearly lies within the boundary region) translates along the crystal, reflecting the advancement of the new pentadecane guest molecules through the crystal and displacement of the original 1,8-dibromooctane guest molecules.

While such $R_{N,T}(X,t)$ plots provide a clear qualitative demonstration of the occurrence and progress of the guest exchange process, arising from the fact that $R_{N,T}$ depends on the relative

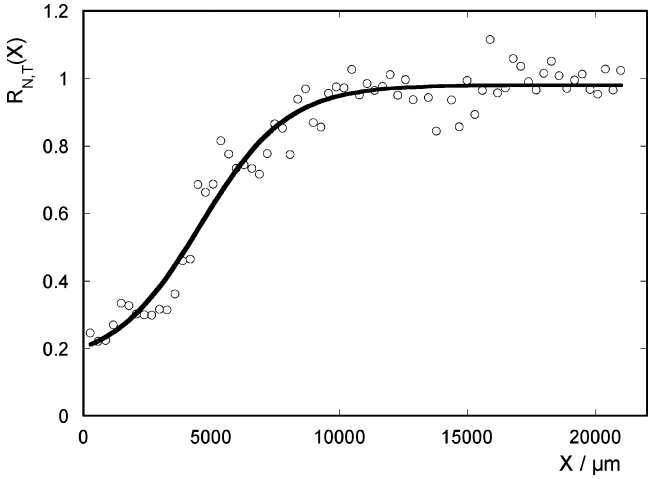

Figure 4. Variation of $R_{N,T}$ as a function of position X along the tunnel at a fixed value of time (372 min) after commencement of the guest exchange process.

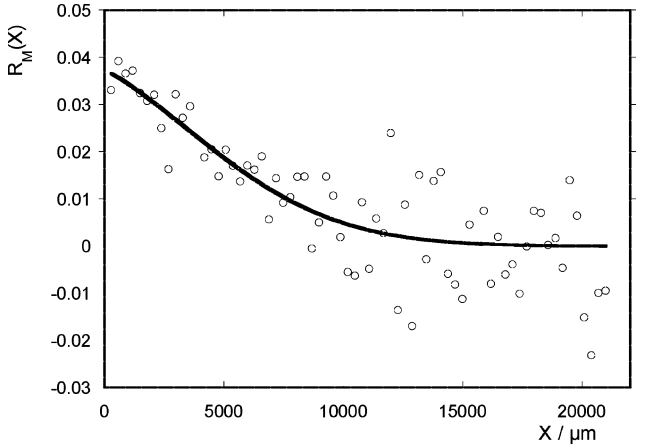

Figure 5. Variation of R_M as a function of position X along the tunnel at a fixed value of time (372 min) after commencement of the guest exchange process. Results obtained from the same set of Raman spectra used to construct Figure 4.

amounts of 1,8-dibromooctane and pentadecane guest molecules within a given region of the crystal, it is important to emphasize that the value of $R_{N,T}$ is also sensitive to changes that may occur in the relative amounts of trans and gauche end-group conformations for the 1,8-dibromooctane guest molecules. In the present paper, we focus on this specific aspect of the guest exchange process.

3. Experimental Details

Confocal Raman microspectrometry[26] was carried out using a Labram II spectrometer (Jobin-Yvon), an Ar/Kr 2018 Spectra-Physics laser (514.5 nm) and a grating of 1800 lines/mm (spectral resolution ca. 6 cm^{-1}). The laser was focused on the sample through a microscope with a 10× Olympus objective of 0.25 numerical aperture and confocal pinhole diameter of 140 μm. The diameter of the probed area was 10 μm (defining the radial resolution of the experiment).

Crystals of the 1,8-dibromooctane/urea inclusion compound were prepared using standard procedures, as follows. An excess amount of 1,8-dibromooctane (excess with respect to the expected molar guest/host ratio in the inclusion compound) was added to a saturated solution of urea in methanol at 50 °C. The solution was cooled to 20 °C over a period of several days. Needle-shaped crystals with long hexagonal needle morphology were collected, with length ca. 10−30 mm and "diameter" ca. 1−2 mm. The crystals were washed with 2,2,4-trimethylpentane prior to the Raman experiments in order to remove any guest molecules adhering to their external surfaces.

In the confocal Raman microspectrometry experiments discussed below, a single crystal (dimensions ca. $1 \times 1 \times 30$ mm^3) of the 1,8-dibromooctane/urea inclusion compound was attached (using Araldite as a sealing system) to a reservoir containing liquid pentadecane (Figure 2). The single crystal and reservoir were mounted on the *XY*-motorized table of the confocal Raman microscope. The laboratory reference frame is defined in Figure 2, with the *Z*-axis collinear to the direction of the incident laser beam. The scattered light was collected in the same direction as the incident light (backscattering geometry). The long axis (tunnel direction) of the needle-shaped crystal was aligned parallel to the X axis of the reference frame and polarized spectra were recorded [$(Z(XX)\bar{Z})$ and $(Z(XY)\bar{Z})$ in Porto notation;[27] note that no polarizer was used for the backscattered light].

Analysis was performed at a depth $Z = 300$ μm beneath the upper surface of the crystal with axial resolution of 200 μm. The Raman spectra were collected in scans along the X axis with a step size of 300 μm and a total scan range of 20 mm; six separate scans of this type were carried out at Y coordinates separated by 100 μm (the "width" along Y of each scan, determined by the spatial resolution, was ca. 10 μm). The acquisition time for each Raman spectrum was 12 s, and the time to record each scan was ca. 14 min. The time to record the complete Raman micrograph of the probed area was thus about 80 min, which is significantly shorter than the overall time scale of the guest exchange process.

The intensities of bands in the Raman spectra were determined by numerical integration of the peak area, with the baseline defined as a straight line between the specified extrema of the spectral window; for a given Raman band, the same extrema of the spectral window were defined for all spectra. As discussed in section 4, all analysis carried out in this paper is based on *relative* intensities of Raman bands, and in particular, the variation in the *relative* intensities of Raman bands as function of position (X) along the tunnel direction and as a function of time. In all cases, the results are averaged over the six independent scans carried out at fixed values of Y.

4. Results

The variation of $R_{N,T}$ as a function of position X at a fixed value of time after commencement of the guest exchange process is shown in Figure 4, demonstrating the sigmoidal distribution discussed above. For the same set of Raman spectra used to construct Figure 4, the ratio $R_M = I(CH_3)/I(CN)$ of the integrated intensities [denoted $I(CH_3)$ and $I(CN)$, respectively] of the $r(CH_3)$ and $\nu_s(CN)$ Raman bands is shown in Figure 5 (we note that there is significant scatter of the R_M data due to the very low intensity of the $r(CH_3)$ band in the Raman spectrum). It is clear that R_M also exhibits a sigmoidal distribution (but in the opposite sense to $R_{N,T}$), with R_M increasing as X decreases within the boundary region, reflecting the displacement of the original 1,8-dibromooctane guest molecules by pentadecane guest molecules in the guest exchange process. This increase in R_M as X decreases within the boundary region is associated with the decrease in $R_{N,T}$ as X decreases in the same region, shown in Figure 4, and it is clear that this variation in $R_{N,T}$ within the boundary region reflects the decrease in the absolute amount of 1,8-dibromooctane guest molecules due to the guest-exchange process. These conclusions are also corroborated by other measured intensity ratios (not shown); in particular, $I(CBr_T)$/

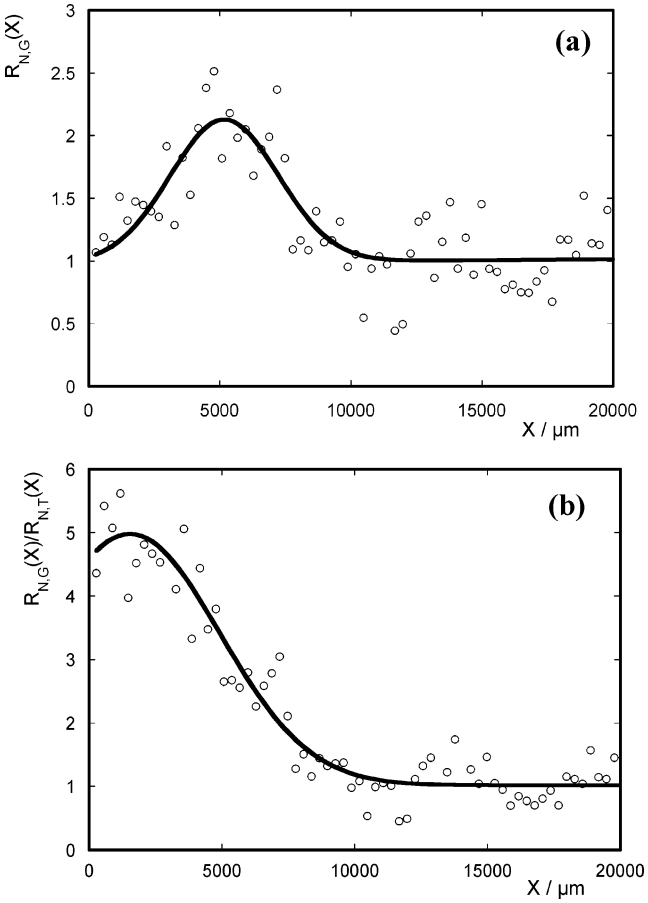

Figure 6. Variation of (a) $R_{N,G}$ and (b) $R_{N,G}/R_{N,T}$ as a function of position X along the tunnel at a fixed value of time (372 min) after commencement of the guest exchange process. Results obtained from the same set of Raman spectra used to construct Figures 4 and 5.

I(NCO) and $I(CH_3)/I$(NCO), where I(NCO) is the intensity of the band at ca. 535 cm^{-1} for the urea NCO bending mode. These other intensity ratios also show that the decrease in $I(CBr_T)/I$(NCO) on moving to lower values of X across the boundary region is associated with an increase in $I(CH_3)/I$(NCO) across the same region.

Next, we consider the C−Br stretching vibration for the gauche end-group conformation of the 1,8-dibromooctane guest molecules. The normalized ratio $R_{N,G}$ is defined as $R_{N,G} = R_G/R_{G,0}$, where $R_G = I(CBr_G)/I$(CN) and $R_{G,0}$ is the value of R_G for the original crystal of 1,8-dibromooctane/urea before commencement of the guest exchange process. Clearly, the value of $R_{N,G}$ reflects the relative amount of 1,8-dibromooctane guest molecules with the gauche end-group conformation (relative to the amount in the original 1,8-dibromooctane/urea inclusion compound) and is directly analogous to the quantity $R_{N,T}$ used to assess the relative amount of 1,8-dibromooctane guest molecules with the trans end-group conformation. The variation of $R_{N,G}$ versus position X for a fixed value of time after commencement of the guest exchange process is shown in Figure 6a. Importantly, the $R_{N,G}$ data, while relatively "noisy" (due to the low absolute intensity $I(CBr_G)$ of the $\nu(CBr_G)$ Raman band), show a distinct increase in $R_{N,G}$ as X decreases within the boundary region. Given, as discussed above, that the absolute amount of 1,8-dibromooctane guest molecules decreases as X decreases across this region, this result suggests that there is a marked increase in the proportion of 1,8-dibromooctane guest molecules with the gauche end-group conformation in the boundary region. This conclusion is illustrated more directly

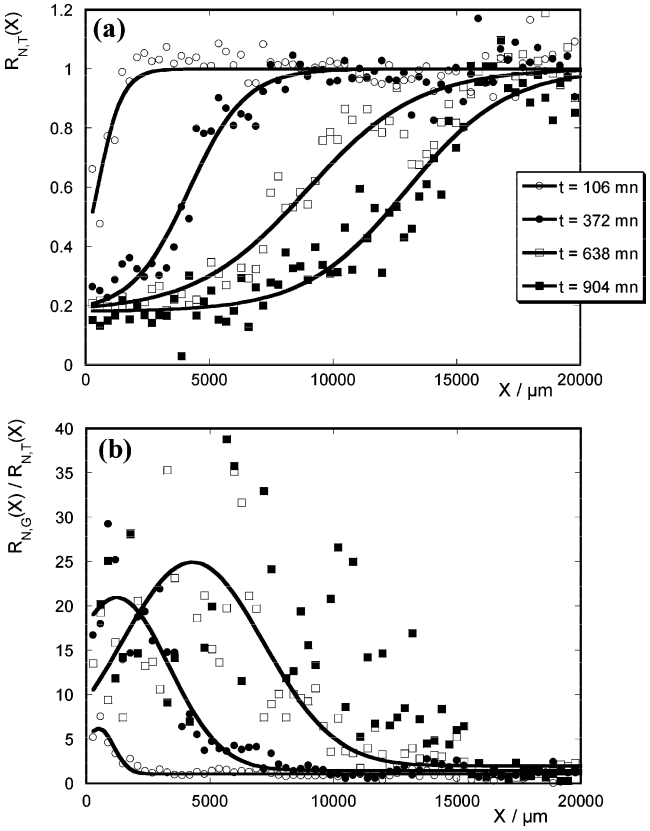

Figure 7. Evolution of (a) $R_{N,T}$ versus X and (b) $R_{N,G}/R_{N,T}$ versus X as a function of time (t) during the guest exchange process (open circles, $t = 106$ min; filled circles, $t = 372$ min; open squares, $t = 638$ min; filled squares, $t = 904$ min). Because of the significant scatter of the data for $t = 904$ min in part b, no fitted line is shown.

by considering the ratio $R_{N,G}/R_{N,T}$, which is independent of the absolute amount of 1,8-dibromooctane guest molecules in a given region within the crystal (note that, by definition, $R_{N,G}/R_{N,T} = 1$ for the original crystal of the 1,8-dibromooctane/urea inclusion compound). The variation of $R_{N,G}/R_{N,T}$ as a function of position X for a fixed value of time after commencement of the guest exchange process is shown in Figure 6b, from which it is clear that the gauche/trans ratio for the 1,8-dibromooctane guest molecules increases significantly within the boundary region. It is important to note that the value of $R_{N,G}/R_{N,T}$ does not directly indicate the relative amounts of 1,8-dibromooctane guest molecules with gauche and trans end-group conformations, as the $\nu(CBr_G)$ and $\nu(CBr_T)$ modes are polarized differently[24] (in particular, see Figure 11B in ref 24). Nevertheless, the value of $R_{N,G}/R_{N,T}$ provides a reliable indication of qualitative trends in the relative amounts of gauche and trans end-group conformations, and the increase in $R_{N,G}/R_{N,T}$ from 1 for the original 1,8-dibromooctane/urea crystal to a value of ca. 5 within the boundary region represents a significant change in the conformational properties of the guest molecules within this region.

The variation of $R_{N,T}$ as a function of position X for different fixed values of time after commencement of the guest exchange process is shown in Figure 7a, and the corresponding variation of $R_{N,G}/R_{N,T}$ as a function of position X at the same fixed values of time is shown in Figure 7b. It is clear that the region with increased gauche/trans ratio moves through the crystal as the boundary region advances through the crystal and is associated specifically with this region. Thus, in the limiting regions of the sigmoidal distribution, the value of $R_{N,G}/R_{N,T}$ is close to that in the original crystal of the 1,8-dibromooctane/urea inclusion

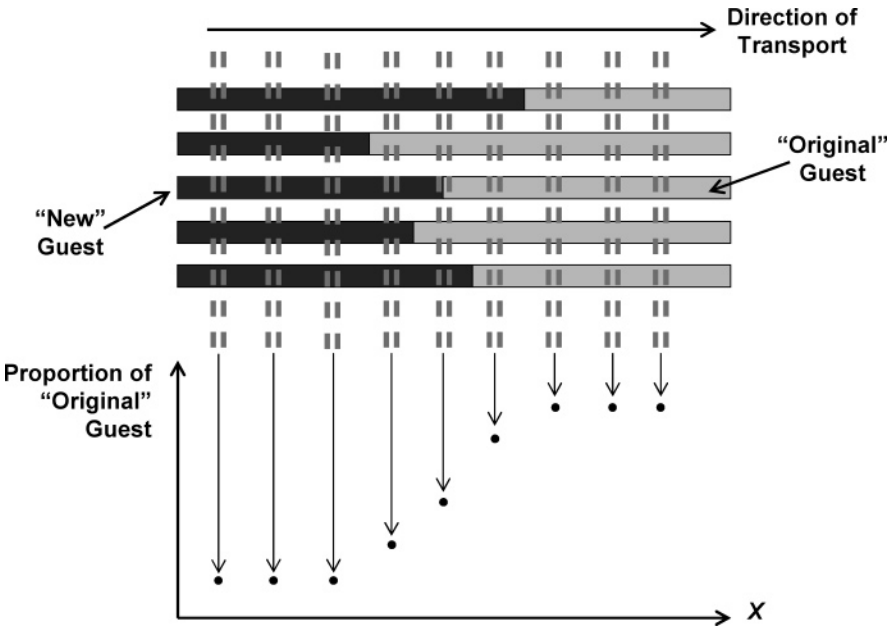

Figure 8. Schematic illustration of the origin of a sigmoidal distribution for the proportion of original guest molecules in a tunnel inclusion compound during guest exchange (which occurs from left to right). Five individual tunnels are shown (horizontal). In each individual tunnel, the distribution of the original (light gray) and new (dark gray) guest molecules is described by a step-function. The "step" between the original and new guest molecules occurs, in general, at a different value of X (denoted X_b in the text) in each tunnel. The vertical dashed lines indicate the region of sampling by the laser probe, involving averaging over all tunnels shown.

compound used in the experiment (although we note that, in the pentadecane-rich region, the measurement of $R_{N,G}/R_{N,T}$ has low reliability due to the diminished absolute intensities of both the $\nu(CBr_G)$ and $\nu(CBr_T)$ Raman bands).

5. Discussion

It is clear from the results presented above that, in the boundary region, there is a significant increase in the proportion of 1,8-dibromooctane guest molecules that have the gauche end-group conformation. To understand the physical basis for this observation, we must first understand the nature of the "boundary region" in the crystal during the guest exchange process. First, we recall (see section 3) that the types of measurements shown in Figures 4−7 represent an averaging over a large number of tunnels (in the Y and Z directions), as dictated by the spatial resolution of the probe, and for a given tunnel, each measurement represents an averaging over a length of ca. 10 μm along the tunnel (X direction).

For an *individual tunnel*, it is reasonable to suppose that, along the complete length of the tunnel, there is a region (at higher X values) containing only the original 1,8-dibromooctane guest molecules and a region (at lower X values) containing only the new pentadecane guest molecules; between these regions, there is a sharp boundary at a specific point (X_b) along the tunnel. A plot of the number of 1,8-dibromooctane guest molecules (per unit length of tunnel) versus X *for an individual tunnel* would be a step-function, with the step occurring at $X = X_b$. Within an individual tunnel, there is therefore no "boundary region" containing *both* the original and new guest molecules. In general, at a given value of time, different tunnels within the region of the crystal probed by the Raman microspectrometry experiments will have different values of X_b, and it is reasonable to propose that there is a well-defined distribution of X_b values for the set of tunnels probed. On averaging over these tunnels, it is reasonable to expect a sigmoidal distribution for the proportion of 1,8-dibromooctane guest molecules versus X. A schematic diagram of this situation is shown in Figure 8. Thus, the boundary region containing both the original and new guest molecules, as observed in results such as Figures 4−7, arises because of the distribution of X_b values for different tunnels and because the sampling in the Raman microspectrometry experiments involves averaging over a large number of tunnels. The boundary region in such plots represents an averaging over some tunnels in which only the region of original guest molecules is probed (i.e., tunnels with X_b values lying outside the probed region on the high-X side), some tunnels in which only the region of new guest molecules is probed (i.e. tunnels with X_b values lying outside the probed region on the low-X side) and other tunnels in which the step at X_b lies within the probed region.

To understand the fact that there is an increase in the proportion of 1,8-dibromooctane guest molecules with the gauche end-group conformation in the boundary region, we consider first the situation in an individual tunnel. The advancing front of the new guest molecules along the tunnel applies a force (pressure) on the original guest molecules, and in response to this force, the original guest molecules may be compelled to adopt a different conformational state from that observed in the original 1,8-dibromooctane/urea inclusion compound (under ambient conditions). In the present case, we propose that such local pressure applied on the 1,8-dibromooctane guest molecules leads to an increase in the proportion of gauche end-group conformations. It has been established previously[24] that, for the 1,11-dibromoundecane/urea inclusion compound at elevated pressure (from 1 bar to 6 kbar), there is a marked increase in the proportion of gauche end-groups, and similar behavior may be anticipated for 1,8-dibromooctane guest molecules. We note that the effective length (including consideration of van der Waals radii) of an α,ω-dibromoalkane molecule with two gauche end-groups (but otherwise with an all-trans alkyl chain) is ca. 3.0 Å shorter than the length of the corresponding α,ω-dibromoalkane molecule with two trans end-groups, and thus a higher density of packing of the 1,8-dibromooctane guest molecules per unit length of tunnel may be achieved by

increasing the proportion of gauche end-groups. Clearly, the ability to adopt a higher packing density is favorable under conditions of the type of local pressure discussed above. Nevertheless, we note that the formation of a gauche end-group conformation has unfavorable consequences with regard to the intramolecular potential energy of the guest, and possibly also with regard to the host−guest interaction energy (the bromine atom in the gauche end-group protrudes directly into the wall of the tunnel and may give rise to a distortion of the urea tunnel structure in the local vicinity).

Because of the averaging over several tunnels (a consequence of the spatial resolution of the Raman microspectrometry technique used in the present work), we cannot at this stage assess the spatial extent of the region *in a given tunnel* over which the 1,8-dibromooctane guest molecules have an increased proportion of gauche end-groups. Presumably, at sufficient distance from the boundary region, mechanisms will operate to relax the pressure generated locally at the boundary region. We note that, in the region of the exchanging crystal that contains only the original 1,8-dibromooctane guest molecules (i.e., on the high-*X* side of the boundary region), the proportion of gauche end-groups is similar to that in the original crystal before commencement of the guest exchange process, so it is clear that the increased proportion of gauche end-groups is not transmitted throughout the whole tunnel in the exchanging crystal. From the present results, we are not able to quantify the actual magnitude of the local pressure generated at the boundary region, nor to assess whether the guest exchange process is associated with any change in the conformational properties of the new pentadecane guest molecules, but these issues are the focus of our continuing research program in this field.

It is interesting to note (see Figure 4) that complete exchange of guest molecules does not occur, even at long values of time (i.e., at the end of the experiments, over ca. 15 h), and that the proportion of 1,8-dibromooctane guest molecules does not fall to zero even in the pentadecane-rich region of the crystal (i.e., on the low-*X* side of the boundary region). It is reasonable to suggest that a proportion of the original guest molecules may be unable to take part in the guest exchange process as a consequence of structural defects, which may impede the transport of the guest molecules in some tunnels. In addition to this explanation, the results presented here may allude to other possible mechanisms for impeding the transport of guest molecules in certain tunnels; for example, the increase in the proportion of 1,8-dibromooctane guest molecules that have gauche end-groups will undoubtedly lead to local distortions of the wall of the urea tunnel, and such distortions in a given tunnel might influence significantly the transport of guest molecules in neighboring tunnels (for example, the local distortion to accommodate a gauche end-group in a given tunnel might represent a local widening of the tunnel in the region of the end-group; recalling that a pair of neighboring tunnels share a common tunnel wall (see Figure 1), such a distortion could cause a constriction in a neighboring tunnel).

Finally, on the basis of the observations reported here, we may anticipate that the guest exchange process might be facilitated for those guest molecules (as the original guest) that are readily able to adopt gauche end-group conformations within the urea tunnel structure, and investigation of this issue is also part of our ongoing research in this area.

Acknowledgment. We are grateful to the European Union (Marie Curie Training Fellowship to J.M.R.) and to Cardiff University (studentship to J.M.R.) for financial support and to D. Talaga and J.L. Bruneel (LPCM) for technical assistance.

References and Notes

(1) Preston, G. M.; Carroll, T. P.; Guggino, W. B.; Agre, P. *Science* **1992**, *256*, 385.
(2) Doyle, D. A.; Morais Cabral, J.; Pfuetzner, R. A.; Quo, A.; Gulbis, J. M.; Cohen, S. L.; Chait, B. T.; MacKinnon, R. *Science* **1998**, *280*, 69.
(3) MacKinnon, R. *FEBS Lett.* **2003**, *555*, 62.
(4) Agre, P. *Biosci. Rep.* **2004**, *24*, 127.
(5) MacKinnon, R. *Angew. Chem. Int. Ed.* **2004**, *43*, 4265.
(6) Agre, P. *Angew. Chem. Int. Ed.* **2004**, *43*, 4278.
(7) Karger, J.; Ruthven, D. M. *Diffusion in Zeolites and other Microporous Solids*; Wiley: New York, 1992.
(8) Thomas, J. M. *Angew. Chem. Int. Ed.* **1999**, *38*, 3588.
(9) Lee, S. B.; Martin, C. R. *J. Am. Chem. Soc.* **2002**, *124*, 11850.
(10) Hod, O.; Rabani, E. *Proc. Natl. Acad. Sci.* **2003**, *100*, 14661.
(11) Kalra, A.; Garde, S.; Hummer, G. *Proc. Natl. Acad. Sci.* **2003**, *100*, 10175.
(12) Wei, C. Y.; Srivastava, D. *Phys. Rev. Lett.* **2003**, *91*, Art. No. 235901.
(13) Lee, K. H.; Sinnott, S. B. *J. Phys. Chem. B* **2004**, *108*, 9861.
(14) Nednoor, P.; Chopra, N.; Gavalas, V.; Bachas, L. G.; Hinds, B. J. *Chem. Mater.* **2005**, *17*, 3595.
(15) Fetterly, L. C. *Non-Stoichiometric Compounds*; Mandelcorn, L., Ed.; Academic Press: New York, 1964; p 491.
(16) Takemoto, K.; Sonoda, N. *Inclusion Compounds*; Atwood, J. L., Davies, J. E. D.; MacNicol, D. D., Eds.; Academic Press: New York, 1984; Volume 2, p 47.
(17) Hollingsworth, M. D.; Harris, K. D. M. *Comprehensive Supramolecular Chemistry*; MacNicol, D. D., Toda, F., Bishop, R., Eds; Pergamon Press: 1996; Volume 6, pp 177−238.
(18) Harris, K. D. M. *Chem. Soc. Rev.* **1997**, *26*, 279.
(19) Guillaume, F. *J. Chim. Phys. (Paris)* **1999**, *96*, 1295.
(20) Smith, A. E. *Acta Crystallogr.* **1952**, *5*, 224.
(21) Harris, K. D. M.; Thomas, J. M. *J. Chem. Soc. Faraday Trans.* **1990**, *86*, 2985.
(22) Khan, A. A.; Bramwell, S. T.; Harris, K. D. M.; Kariuki, B. M.; Truter, M. R. *Chem. Phys. Lett.* **1999**, *307*, 320.
(23) Marti-Rujas, J.; Desmedt, A.; Harris, K. D. M.; Guillaume, F. *J. Am. Chem. Soc.* **2004**, *126*, 11124.
(24) Smart, S. P.; El Baghdadi, A.; Guillaume, F.; Harris, K. D. M. *J. Chem. Soc., Faraday Trans.* **1994**, *90*, 1313.
(25) El Baghdadi, A.; Guillaume, F. *J. Raman Spectrosc.* **1995**, *26*, 155.
(26) Bruneel, J. L.; Lassègues, J. C.; Sourisseau, C. *J. Raman Spectrosc.* **2002**, *33*, 815.
(27) Damen, T. C.; Porto, S. P. S.; Tell, B. *Phys. Rev.* **1966**, *142*, 570.